An enhanced stochastic optimization in fracture network modelling conditional on seismic events

S. Seifollahi, P.A. Dowd and C. Xu

School of Civil, Environmental and Mining Engineering, The University of Adelaide,

Adelaide, SA 5005, Australia

Abstract:

This paper presents an approach to modelling fracture networks in hot dry rock geothermal reservoirs. A detailed understanding of the fracture network within a geothermal reservoir is critically important for assessments of reservoir potential and optimal production design. One important step in fracture network modelling is to estimate the fracture density and the fracture geometries, particularly the size and orientation of fractures. As fracture networks in these reservoirs can never be directly observed there is significant uncertainty about their true nature and the only feasible approach to modelling is a stochastic one. We propose a global optimization approach using simulated annealing which is an extension of our previous work. The fracture model consists of a number of individual fractures represented by ellipses passing through the micro-seismic points detected during the fracture stimulation process, i.e. the fracture model is conditioned on the seismic points. The distances of the seismic points from fitted fracture planes (ellipses) are, therefore, important in assessing the goodness-of-fit of the model. Our aims in the proposed approach are to formulate an appropriate objective function for the optimal fitting of a set of fracture planes to the micro-seismic data and to derive an efficient modification scheme to update the model parameters. The proposed objective function consists of three components: orthogonal projection distances of the seismic points from the nearest fitted fractures, the amount of fracturing (fitted fracture areas) and the volumes of the convex hull of the associated points of fitted fractures. The functions used in the model update scheme allow the model to achieve an acceptable fit to the points and to converge to acceptable fitted fracture sizes. These functions include two groups of proposals: one for updating fracture parameters and the other for determining the size of the fracture network. To increase the efficiency of the optimization, a spatial clustering approach, the Distance-Directional Transform, was developed to generate parameters for newly proposed fractures. A simulated dataset was used as an example to evaluate our approach and we compared the results to those derived using our previously published algorithm on a real dataset from the Habanero geothermal field in the Cooper Basin, South Australia. In a real application, such as the Habanero dataset, it is difficult to determine definitively which algorithm performs better due to the many uncertainties but the number of association points, the number of final fractures and the error are three important factors that quantify the effectiveness of our algorithm.

Keywords: Fracture Network Modelling, Global Optimization, Simulated Annealing, Conditional Modelling, Seismic Events

1. Introduction

Hot dry rock (HDR) geothermal energy has the potential to make a significant contribution to achieving a sustainable energy future. Potential HDR geothermal systems occur in deep underground crystalline rock, where the rock matrix (granite) is almost impermeable and the only viable pathway for geothermal flow is through an engineered fracture network. Understanding the fractures and the fracture

network within the geothermal reservoir is therefore critically important for the design and operation of the system (Brown et al. 1999; Nelson 1982; Tran et al. 2002; Xu et al. 2013).

Earlier mathematical models for fracture networks and flow through them include continuum models that assume a fractured rock mass can be represented as an equivalent porous medium (Hsieh et al. 1985; Long and Witherspoon 1985; Odling 1992; Xing et al. 2009) and discrete fracture networks (DFN) that rely on a detailed description of discontinuity geometry (Dershowitz and LaPointe 1994; Einstein 2003; Mardia et al. 2007a; Mardia et al. 2007b; Tamagawa et al. 2002; Tran et al. 2002; Xu et al. 2007; Xu et al. 2010). In DFN, which provides an approximate representation of the reservoir fracture network, it is very difficult to obtain a reliable description of the fracture geometry as, in most cases, it is impossible to observe or measure fractures directly on any scale relevant to the problem. Studies are generally limited to sparse, small-scale observations (e.g., on drill cores) or indirect measures such as those provided by geophysical surveys or, in the case of engineered geothermal systems (EGS), micro-seismic events generated during the fracture stimulation process. The seismic point cloud can be used not only to determine the geographical extent of the HDR reservoir but also to detect fracture geometry in a fractured reservoir (Xu et al. 2013; Seifollahi et al. 2012). Establishing the discrete fracture network model (DFN) conditioned to this seismic point cloud is a way of creating a more realistic model of a HDR EGS.

The significant uncertainties associated with DFN necessitate a stochastic approach. Stochastic modelling of fracture networks originated in percolation studies (Robinson 1983; Sahimi 1993) and was promoted in the 1980s for its wider application to rock engineering (e.g., Long et al. 1982; Baecher 1983; Andersson et al. 1984; Dershowitz and Einstein 1988). It is a general approach in which the fracture characteristics, such as size and orientation, are treated as random variables with inferred probability distributions. In the simplest case, once the parameters of the distributions are inferred, the rock fracture model is constructed by Monte Carlo simulation (Xu and Dowd 2010). More realistic models include the spatial variability of the variables in the simulation.

Recently, DFN conditional on two- and three-dimensional data have been proposed; see for example: Fadakar et al. (2013), Mardia et al. (2007a and 2007b), Seifollahi et al. (2012), Seifollahi et al. (2013), Tran (2007), Xu et al. (2013). A Markov Chain Monte Carlo (MCMC) approach was applied to the conditioning of a fracture model to borehole data in a 2D application (Mardia et al. 2007a) and the model was later extended to 3D applications (Mardia et al 2007b). An extension of MCMC to the conditioning of a fracture model to the seismic events was used in Xu et al. (2013) for a data set from the Habanero geothermal field. In this model the number of fractures is fixed in advance and the unknown fracture variables (e.g., size and orientation), are optimized during the MCMC process. In the present work, the number of fractures is also a variable to be optimized during the optimization process. We also extend the work of Seifollahi et al. (2012 and 2013) by including more components in the objective function and introducing more update proposals to improve the conditioning process.

This paper presents a general stochastic model for fracture networks in a fractured HDR reservoir. Two challenging factors in a global optimization problem are the construction of an appropriate objective function and the formulation of an efficient model modification scheme. In our approach, the objective function consists of three components to minimize, respectively, the distances of the points to the fitted fracture model, the amount of fracturing and the volumes of the convex hull of the points associated with fractures. The model modification functions include two categories of proposals. The first category is for updating fracture geometry variables and the second is for adjusting the size of the fracture network (number of fractures). Simulated annealing (SA) is the core of our model in which it is used to minimize the objective function by accepting or rejecting any update proposed by the model modification functions (Seifollahi et al.

2013). To enhance the optimization process, a spatial clustering approach, developed by Seifollahi et al. (2012), and termed the DD-Transform, is used to help determine the fracture geometry. It should be noted that the accuracy of the seismicity detection and the inversion process in deriving the locations of seismic points are not concerns of this paper; readers interested in these topics should consult Baisch et al. (2006).

The paper is organized as follows: In Section 2, we give a description of the model and the problem formulation, with a focus on fracture bandwidth. The fracture bandwidth is an interval around fractures used to weight the objective function to reflect the importance of the locations of the points to the fracture model as well as controlling the number of fractures in the network. In Section 3, we describe the DD-Transform, which determines a solution for the parameters of newly proposed fractures during the optimization process. In Section 4 we present the proposals for updating fracture parameters and for permitting the network to grow or diminish (by pruning), which is followed by details of the proposed model. The performance of the proposed model is illustrated in Section 5 using two validation datasets, first using a simulated dataset and then a real dataset from the Habanero reservoir (Baisch et al. 2006; Xu et al. 2013).

2. Problem formulation

In discrete fracture network modelling, the most common approach is to use simple representations of fractures although it is possible to represent fractures by tortuous surfaces. Common approaches include circular discs, elliptical discs, planar polygons or planes with infinite extents (Mardia et al. 2007b; Seifollahi et al. 2012; Seifollahi et al. 2013; Xu et al. 2013). In the work reported here, we represent a fracture by an ellipse. We consider this to be a simple, but reasonable, approximation to actual fracture surfaces as fractures with curved features can be subdivided into planar regions connected to each other. With this simplification, each fracture can be described by eight parameters, $(x, y, z, \alpha, \beta, \gamma, a, b)$, where x, y and z are the coordinates of the fracture centre, α and β are the dip direction and dip angle of the plane, γ is the rotation angle of the major axis against the dip direction of the ellipse and a and b are the major and minor axes of the ellipse. Xu and Dowd (2010) provide more detailed descriptions of these parameters.

The fracture model consists of a number of fractures each with its associated cluster of seismic points so that each point is associated with one, and only one, fracture in the model. Note that even the 'best' fitted model will not intersect all seismic points but the distances of the points to fracture planes (the orthogonal projection measure) can be used to assess the goodness-of-fit of the fracture model. The final objective function can be written as (Seifollahi et al. 2013):

$$f(w) = \sum_{i=1}^{n_o} \lambda_i f_i(w), \tag{1}$$

where w is a set of unknown fracture variables to be optimized, n_o is the number of objectives and f_i and λ_i are, respectively, the i^{th} objective and its weight. Constructing a proper objective function (i.e., the number of components and their structures) is critical in ensuring the optimization process converges to a solution. The proposed objective function consists of three components as follows.

1. Distances of the points to fracture planes: the summation of the shortest distances of the points to fracture planes is a major component of the objective function (Seifollahi et al. 2013; Xu et al. 2013):

$$f_1(w) \equiv \sum_{j=1}^{m} d_{jk^*}^2 \quad , \qquad k^* = \underset{k}{\operatorname{argmin}}\left(d_{jk}^2\right) \tag{2}$$

where m is the number of points, j and k are the indices of the j^{th} point and k^{th} fracture and d_{jk}^2 is the squared projection distance of the j^{th} point to the k^{th} fracture. When the orthogonal projection of a point does not intersect any fracture ellipse, the point is not associated with any fracture and a penalty value is applied to the point in the calculation of the objective function.

2. The amount of fracturing: the following objective is used (Seifollahi et al. 2013) to achieve a network with an appropriate amount (area) of fracturing:

$$f_2(w) = \sum_{i=1}^{n} \frac{\delta + a_i \times b_i}{1 + m_i} \tag{3}$$

where n is the number of fractures, a_i and b_i are the major and minor axes of the i^{th} fracture, m_i is the number of points associated with the i^{th} fracture and δ is a positive number proportional to the penalty for an outlier (isolated point); $m = \sum_{i=1}^{n} m_i$ and is used later. The function ensures that in any updating of the DFN smaller fractures are favoured (hence a_i and b_i are smaller) and have more associated points (as m_i is greater).

3. The volumes of the convex hulls of the points associated with fractures: An objective function component calculated as the sum of the volumes of the convex hulls constructed from the associated points of fractures:

$$f_3(w) = \sum_{i=1}^{n} \frac{\delta + V_i^{CH}}{1 + m_i} \tag{4}$$

where n is the number of fractures, V_i^{CH} is the volume of a convex hull constructed from the points associated with the i^{th} fracture and m_i and δ are given in Eq. (3). This function deals with the point-to-point association. Minimizing f_3 not only tends to produce fractures with more associated points but also minimizes the distances of points to the fracture model.

The amount of the contribution of each component to the final objective function in (1) can be controlled by different weighting factors λ_i. In our work, weights $\lambda_i, i = 1, 2, 3$, are set as follows: $\lambda_1 = 1$ and λ_2 and λ_3 are fixed in advance based on the value of f_1 in the prior model. In other words, they are set so that the values of $\lambda_2 f_2$ and $\lambda_3 f_3$ are small portions of $\lambda_1 f_1$; here 1% of the value of $\lambda_1 f_1$. The reason for this weighting procedure is that the most important objective is to minimize the associated distances whilst the other two objectives are to ensure that the fitted model satisfies some pre-specified conditions, e.g. generating a model with appropriate fracture sizes. It is noted that other weighting procedures can be used depending on the objective and application; for example, the weighting procedure used in Deutsch and Cockerham (1994) for the average change in absolute value of the components of the objective function and a convex combination of the components of the objective function used in Goovaerts (1998).

Each seismic point is an indication of fracture growth or stimulation and these points are the only data available for modelling the fracture network. Thus, an essential, but not sufficient, criterion for the fracture model is that it should provide the best possible fit to all the seismic points. However, the model may fail to provide a good local fit in some areas or it may generate an unnecessarily high density of fractures. We address this problem (inappropriate fitting) by using weights in the objective function. The weighting procedure is based on the density of fractures; if the density of fractures around a point is large, a small weight is assigned to the corresponding term in the objective function f_1 and a larger weight is assigned for a smaller density. The function f_1, in this case, is written as

$$f_1(w) \equiv \sum_{j=1}^{m} \xi_j d_{jk^*}^2 \quad , \qquad k^* = \underset{k}{\operatorname{argmin}}\left(d_{jk}^2\right) \tag{5}$$

where m, j, k, d_{jk} are defined in (2) and ξ_j is the weight for the j^{th}point in the objective function defined as:

$$\xi_j = \begin{cases} 1/n_j & n_j > 0 \\ 1 & n_j = 0 \end{cases}$$

and n_j is the number of fractures for which the distances of the j^{th} point to the fractures are less than a specified threshold, i.e. for which the j^{th} point lie inside the bandwidth of the fractures.

3. The Distance-Directional Transform

The Distance-Directional Transform (DD-Transform), proposed by Seifollahi et al. (2012), is used to optimize fracture parameter values. It determines five fracture parameters (out of eight): the centre coordinates, (x, y, z), the dip direction and the dip angle of the fracture plane. The three remaining parameters are generated from their respective distributions. The steps of the DD-Transform are as follows, where *D* denotes the set of points.

1. Set $A = 0$, where A is an $m \times 4$ matrix, m is the number of points in D and the four columns contain the number of counts, an index for the point (fracture centre) and two indices, one for dip direction and the other for dip angle.
2. Select a point $p_i \in D, i = 1, \ldots, m$.
3. Initialize $A^i = 0$, where A^i is a $n_k \times n_l$ matrix; n_k and n_l correspond to the number of divisions of the dip direction and dip angle to be considered; here $n_k = 360$ and $n_l = 90$. For $s = 1,2, \ldots$, do the following:
   3.1. Select two distinct points $p_j, p_{j'} \in D, (j, j' \neq i)$.
   3.2. Fit a plane through the points p_i, p_j and $p_{j'}$ and calculate its dip direction and dip angle.
   3.3. Update $(k, l)^{th}$ element of the matrix

$$A_{kl}^i = A_{kl}^i + arctan\left(d_{ij}^{-r} + d_{ij'}^{-r}\right), \tag{6}$$

   where k and l are the indices of the dip direction and dip angle, respectively; $d_{ij}^{-r}, d_{ij'}^{-r}$ are the distances of p_i to p_j and $p_{j'}$; and r is a positive number.
4. Sort A^i and store the highest value and the corresponding indices (i.e. i, k and l) in the i^{th} row of matrix A (i is the index of p_i and k and l are the indices for dip direction and dip angle). If $i \geq m$, go to the next step; otherwise, repeat from step 2.
5. Sort the rows of A in descending order with respect to the values obtained in step 4.
6. The rows of A, in sequence, correspond to the parameters of the best fractures (the last three elements of each row), which are the dip direction, dip angle and the centre (the stored indices) of the fracture.

Using random portions of points in Step 2 and Step 3.1 will reduce the computational time; in our experiments the number of samples used in steps 2 and 3.1 is the minimum of the total number of points (m) and a random integer number between 10 and 20. The r in (6) is a positive real number and we set $r = 0.5$. The $\arctan(.)$ in (6) can take values between 0 and $\pi/2$. When the distance between a pair of points is very small, its impact on the summation (Eq. (6)) will approach its highest value $\pi/2$ and vice versa.

4. The proposed optimization model

Fracture network modelling, conditioned to a seismic point cloud, requires a stochastic approach (Seifollahi et al. 2012; Seifollahi et al. 2013; Xu et al. 2013). The modelling method proposed in this work provides an efficient modification scheme using simulated annealing. The details of the proposals are discussed below, followed by the introduction of the concept of a fracture bandwidth and the presentation of the proposed fracture network model.

4.1 The DFN updating proposals

Two categories of proposals are incorporated in our model. The first category is related to the determination of fracture parameters, including the coordinates of fracture centres, dip direction, dip angle, rotation angle and major and minor axes of the fractures. The second category is related to the determination of a reasonable fracture network size by growing or pruning techniques such as proposing new fractures or removing redundant fractures.

We use simulated annealing to find the solution in the model (Kirkpatrick 1983; Geman and Geman 1984; Seifollahi et al. 2012). Simulated annealing comprises two main iterations: outer and inner iterations. In the outer iteration the temperature, T, which corresponds to absolute temperature in the physical process of annealing, is updated. In order to do so, we take any initial value T_0 for temperature and a number $r \in (0,1)$ and use the following schedule for temperature: $T_{k+1} = r\,T_k,\ \ k = 0,1,2,\ldots$. In inner iterations the current state is modified, in a random way, to generate a new solution (according to the following proposals). If the move reduces the value of the objective function, the transformation to the new state is accepted. If it increases the value of the objective function, the transformation is accepted with an acceptance probability,

$$A_P = min\left(1, exp\left(\frac{-\Delta f}{T}\right)\right), \tag{7}$$

where $\Delta f = f^{new} - f^{old}$, f^{old} is the function value obtained by simulated annealing in the previous iteration and f^{new} is the function value based on the perturbed configuration. More precisely, a random number u from the uniform distribution $U[0,1]$ is generated. If $u \leq A_P$, the perturbed configuration is accepted as a new solution; otherwise the inner iterations are repeated. Note that the point-fracture association is assessed using only distances of the points to the nearest fracture planes. For more details on simulated annealing see Kirkpatrick (1983), Seifollahi et al. (2012) and Seifollahi et al. (2013).

Coordinates of fracture centres

This proposal moves the centre of a candidate fracture towards one of the associated points of the candidate fracture. The candidate fracture, the point and the amount of translation are all chosen at random,

$$(x, y, z) = (x, y, z) + r\text{đ} \tag{8}$$

where đ is the direction of the move from the current state, $\text{đ} \in R^3$, and r is a random step size to determine the amount of translation, $r \in U[0\ 1]$.

Fracture orientation (dip direction, dip angle and rotation angle)

The proposal is processed independently for each variable. For a given variable, a pair of fractures is selected at random and their corresponding variable values are swapped. As no new values of the variable are involved, the distribution of the orientation remains unchanged after this process.

Fracture size (major and minor axes)

This proposal is repeated independently for each feature. For a given feature, a pair of fractures is chosen at random and their corresponding fracture sizes are swapped. The size distribution will remain unchanged after this process.

Joint

The idea of this proposal is the same as that in Seifollahi et al. (2012) in which two existing fractures are replaced by a new one. Here, we introduce a new similarity measure for selecting two candidate replacement fractures; it uses the volumes of convex hulls defined by the associated points. The similarity of two fractures is defined as

$$S\left(H^i, H^j\right) = \frac{V_i^{CH}/(1+m_i) + V_j^{CH}/\left(1+m_j\right)}{V_{i,j}^{CH}/\left(1+m_{i,j}\right)} \tag{9}$$

where V_i^{CH}, V_j^{CH} and $V_{i,j}^{CH}$ are the volumes of convex hulls defined by the associated points of the i^{th}, j^{th} and both fractures respectively, and m_i, m_j and $m_{i,j}$ are the numbers of associated points of the i^{th}, j^{th} and both fractures. The two candidate fractures are the pair of fractures with the highest similarity measure. The DD-Transform is then applied to generate the parameters of the new fracture. The steps of the Joint proposal are:

1. Select the two similar fractures using (9).
2. Apply the DD-Transform to the associated points of both the candidate fractures to find the centre, dip direction and dip angle of a new fracture.
3. Generate the rotation angle and major and minor axes of the new fracture from their distributions.
4. Re-evaluate the point-fracture association given the new fracture.
5. Accept or reject the proposal based on Eq. (7).

Removal

During the optimization process, fractures with a small number of associated points or a low point density (defined as the number of associated points per unit area of the fracture ellipse) are possible redundant fractures and are therefore candidate fractures for possible removal from the fracture network. Two versions are considered:

1. A fracture is chosen based on the lowest density.
2. A fracture is chosen based on the minimum number of associated points.

The candidate fracture is then proposed to be removed from the network. The only computation, in both versions, is assigning the associated points of the removed fracture to other existing fractures. The acceptance or rejection of the proposal is decided on the basis of Eq. (7).

Replacement

This proposal is to replace an existing fracture with a new one (Seifollahi et al. 2012). The DD-Transform plays a key role in determining the candidate fracture as well as proposing the parameters of the new fracture. The steps in this proposal are:

1. Choose an initial subset of candidate fractures based on the maximum associated distances; i.e., for each fracture determine the maximum point-fracture association distance. Select a set of fractures with the maximum association distance greater than the bandwidth threshold.
2. Apply the DD-Transform to the associated points of each initial candidate fracture.
3. Sort the matrix obtained in Step 2 in descending order. The first row then records the coordinates of the centre, dip direction and dip angle of the new fracture.
4. Generate the other three parameters of the new fracture from their distributions.
5. Replace the fracture corresponding to the associated points with the new one.
6. Accept or reject the proposal based on the probability (7).

Birth

This proposal follows similar steps to the Replacement proposal except for Step 5 in which the candidate fracture is not removed, effectively resulting in the addition of a new fracture. The new fracture is chosen so that the difference between the orientation parameters of the new fracture and the old one is significant (as defined by a threshold); the threshold is set to 5 degrees. In the Replacement proposal, there is no such limitation for generating a new fracture.

Split

This proposal is similar to the Birth proposal except that the candidate fracture is replaced by two new fractures generated by applying the DD-Transform to the points associated with the candidate fracture. This proposal is also similar to the split proposal in Seifollahi et al. (2012). The parameters of the two new fractures, except the rotation angle and the size, are determined by the DD-Transform. The rotation angle and the size of new fractures are generated from their distributions. Similar to the Birth proposal, the difference between the orientations of the two new fractures should be significant as defined by a threshold.

4.2 The Learning Algorithm

In this section, we present the steps used in our approach to generate a general stochastic fracture network model conditioned to a point cloud with a strong emphasis on fracturing (fracture sizes and the number of fractures). In the initialization step (Step 1), a prior model, $\{H^i\}_{i=1}^{n}$, of the fractures is generated, where H^i is an ellipse representing the i^{th} fracture and n is the number of fractures. The centres of the initial fractures are assigned randomly to the seismic points. The size and orientation are generated using random sampling from their specified distribution functions. The prior model is then optimized using the proposals described above. First, the fracture parameters are updated (steps 2 and 3) and then the number of fractures is adjusted using the growing/pruning proposals (steps 5-7). After each proposal, the associations of the points are determined using their (nearest) distances from fractures. The total function value is calculated from the point-fracture association and the acceptance or rejection of proposals is decided on the basis of the probability ratio (7). The algorithm terminates when the stopping criteria (SC) are met; here when a pre-

specified large number of iterations has been completed or when the temperature parameter has been reduced to a specified threshold value.

Algorithm. Stochastic optimization for DFN

1. Initialize n random fractures $\{H^i\}_{i=1}^{n}$, where n is an integer number, $n < m$, and m is the number of seismic events.
2. Update the centres of fractures: select a subset of fractures $\{H^j\}_{j=1}^{n_s}$ at random from the network. For each fracture, update its centre by (8). If SC are met, terminate the algorithm.
3. For each of the remaining parameters, i.e., $4 \leq l \leq 8$: select two distinct subsets of fractures $\boldsymbol{H_1}$ and $\boldsymbol{H_2}$ at random from the network. Select $(H_1, H_2) \in \boldsymbol{H_1} \times \boldsymbol{H_2}$ and swap their l^{th} parameter using simulated annealing. If SC are met, terminate the algorithm.
4. Generate a random number $j \in Z^+$ where Z^+ stands for positive integer numbers.
5. If $j = 2k$ (even number)
   5.1 Apply joint proposal. If SC are met, terminate the algorithm.
   5.2 Apply removal proposals. If SC are met, terminate the algorithm.
6. If $j = 2k + 1$ (odd number)
   6.1 Apply birth proposal. If SC are met, terminate the algorithm.
   6.2 Apply split proposal. If SC are met, terminate the algorithm.
7. Apply replacement proposal. If SC are met, terminate the algorithm.
8. Repeat from Step 2.

5. Experiments

To evaluate the proposed method, we consider two three-dimensional examples. The first example is a simulated dataset and the second is a real dataset from the Habanero geothermal reservoir in South Australia.

5.1. A simulated dataset

This dataset was generated in three steps. First we generate a set of fractures with centres in $[1,10]\times[1,10]\times[1,5]$. The completely known fracture set has the following parameters. The dip direction, dip angle and rotation angle of fractures are drawn from uniform distributions on the following intervals:

$$\alpha \sim U(0,2\pi), \quad \beta \sim U(-\pi/2, \pi/2), \quad \gamma \sim U(-\pi, \pi)$$

The orientation of the major axis follows a lognormal distribution:

$$a \sim logn(\mu_a, \sigma_a)$$

where μ_a and σ_a are the distribution parameters with corresponding Gaussian distribution mean and variance of 1 and 2, respectively. The minor axis is generated from $b \sim a\times(1-u)$ where $u \in U[0,1]$.

A number of points from each fracture are generated at random; the larger the fracture, the greater the number of points generated (i.e., the number of points is proportional to the size of fracture). Given the fracture representation as an ellipse, a set of initial points are regularly sampled from the ellipse. Each sample point is considered as a point between two randomly selected points of the set. Although there is a rich

literature of statistical sampling of point process (Cressie, 1993) for spatial data, our focus here is on stochastic optimisation.

Finally, noise, from a uniform distribution, is added to each point coordinate value (through the normal vector of the fracture plane) to create a dataset resembling reality. Fig.1a and Fig.1b show a set of known fractures (68 fractures) and the simulated point cloud (2133 points). The aim now is to reconstruct the fractures from the simulated point cloud.

Fig. 1c shows the prior model with 33 initial random fractures. This prior model was generated as follows. For each point of the point cloud, if the distance of the point to the fracture model is greater than a specified threshold (proportional to the penalty used for outliers), a new fracture is generated and centred on the point; here the threshold is set to 2. The other fracture parameters (orientation and size) are generated from their respective distributions as discussed above. Fig. 1d shows the final model, i.e. the output after completing the optimization process described in Algorithm 2. In Fig. 1d the total number of fractures in the final model is 64 which is a close match to the 68 in the actual set of fractures.

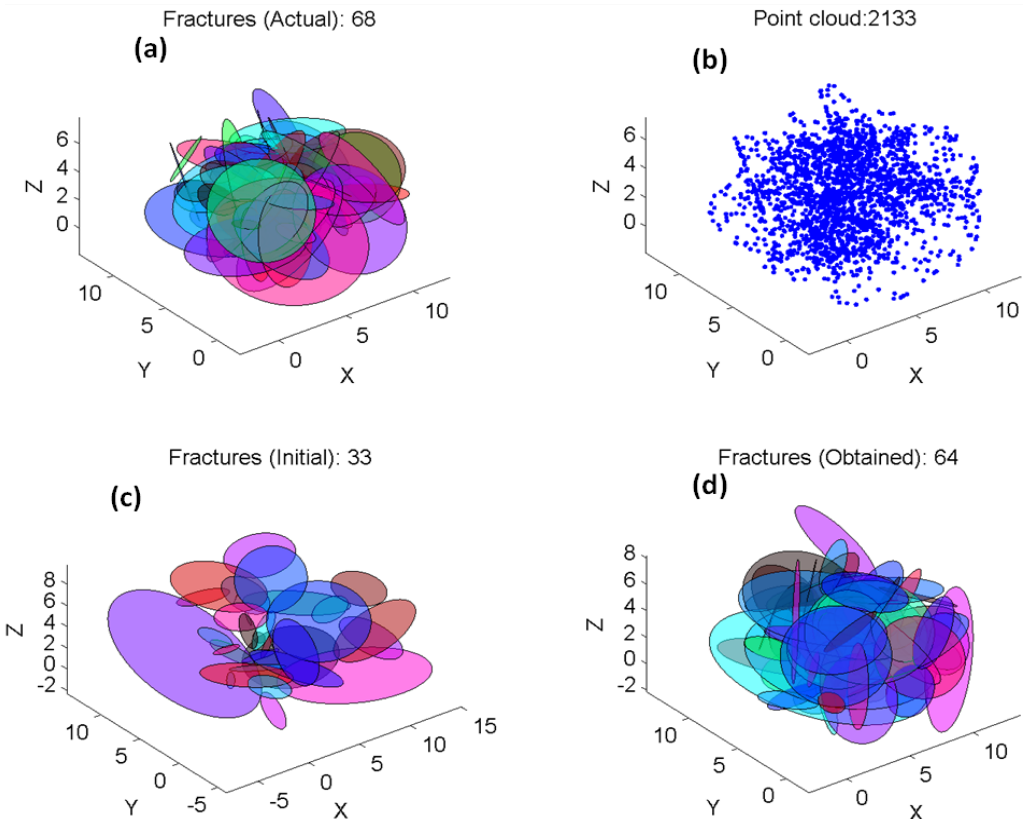

Figure 1. Artificial dataset: a) simulated fractures; b) sampled points; c) prior map; d) final model after optimization

Fig. 2a-2c show the point-fracture associations related to the actual, prior and final fracture models, respectively. In the prior map there are three fractures with more redundant associated points and in the final map these are split into smaller fractures. Fig. 2d represents the noise added to the dataset, i.e. distances of the points from the actual fracture map. Fig. 2e and Fig. 2f show the distribution of the distances of points to the fracture planes in the prior and final model respectively, which highlight the effectiveness of the proposed model.

Fig 3a shows the variation in the number of fractures during the optimization process. Fig. 3b-3c show the objective function values f_2 and f_3 without weights in (1). Fig 3b shows almost the same trend as Fig 3a since increasing the number of fractures increases the area of fracturing. The total objective function value is shown in Fig. 3d which shows a significant decline from earlier iterations and becoming more stable as the number of iterations increases.

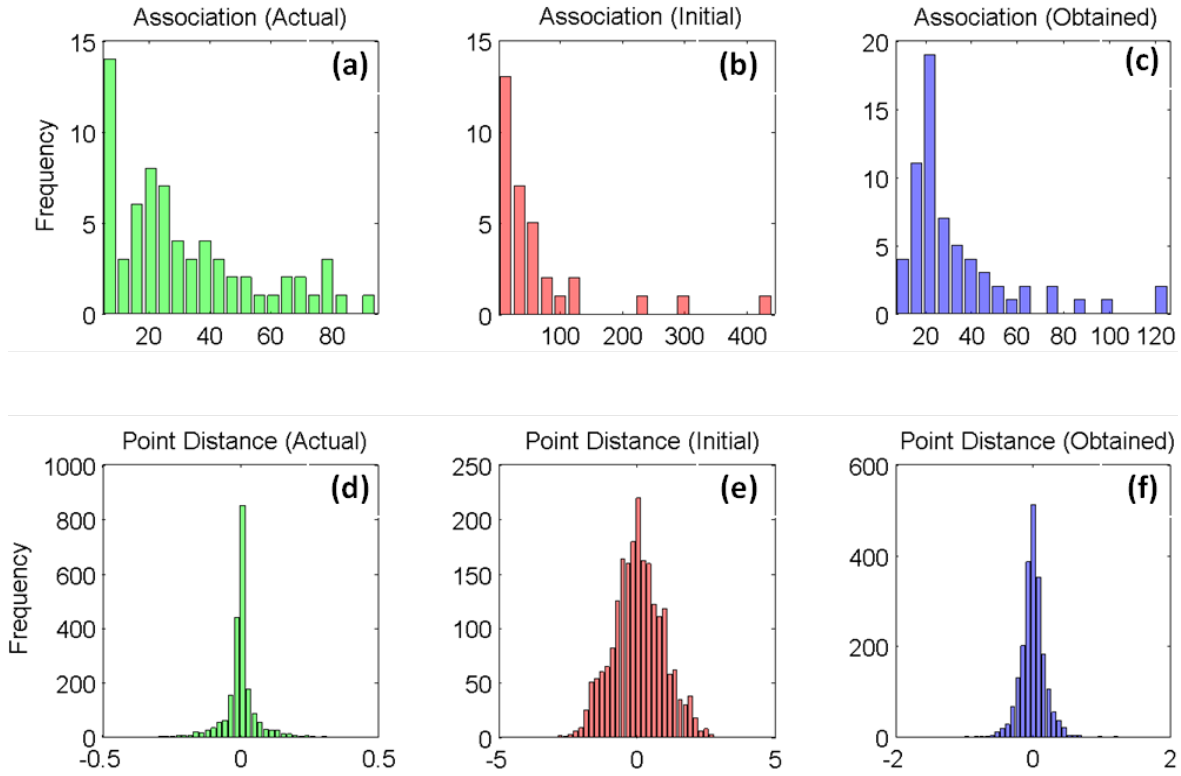

Figure 2. Results for the artificial dataset: a)-c) the point-fracture associations for the actual, initial and obtained fractures; d)-f) the distances of points to the actual, initial and obtained fracture planes.

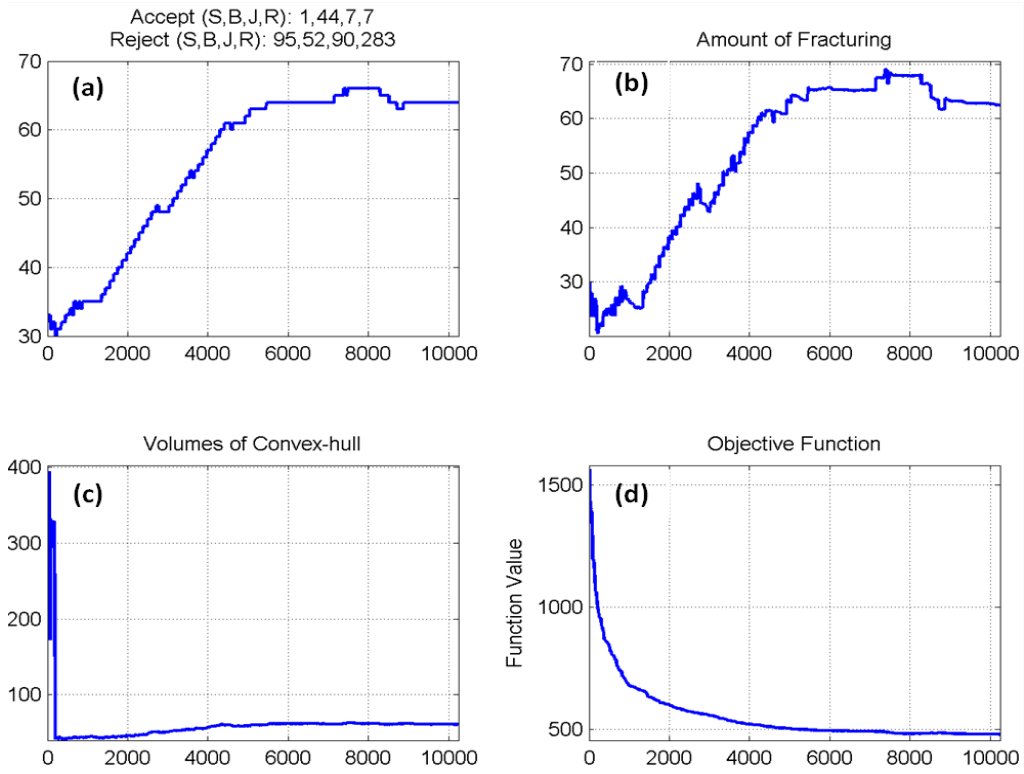

Figure 3. Results for the artificial dataset: a) the variation of #fractures; b) the amount of fracturing (i.e. f_2); c) the volumes of the convex hulls of the associated points (i.e. f_3);d) the total objective function values.

Fig. 4a-4c show the distributions of major axes of fractures in actual, prior and final maps, respectively, and Fig. 4d-4f show the distributions of minor axes for the same maps. The sensitivity of the model to the number of fractures in the initial map is shown in Fig. 5 using 30 independent simulations. The number of fractures in the initial map is between 15 and 50 and the number of fitted fractures after optimization, except in three out of 30 simulations, is between 65 and 80. There is no relationship between the number of fractures in the initial and final maps implying that the model is not sensitive to the number of initial fractures.

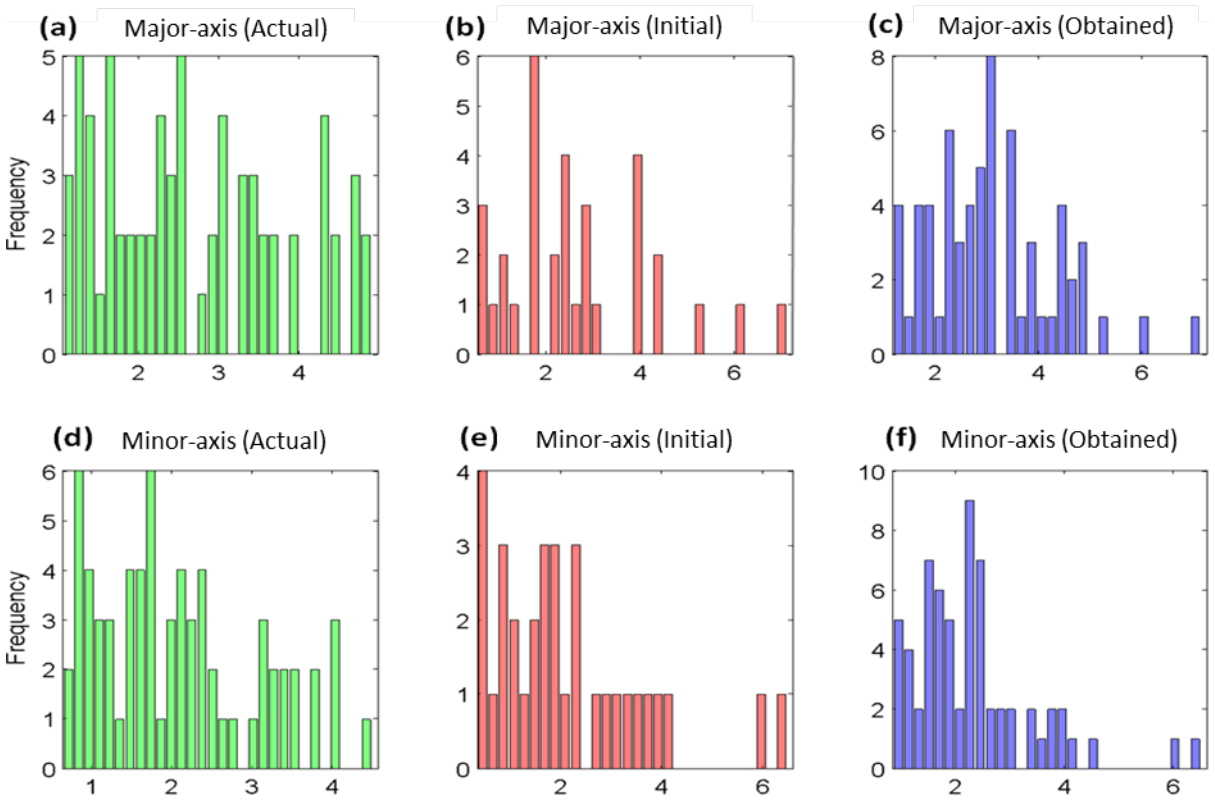

Figure 4. Results for the artificial dataset: a)-c) the distributions of major-axis for the actual, prior and final maps; d)-f) the distributions of minor axis for the same maps.

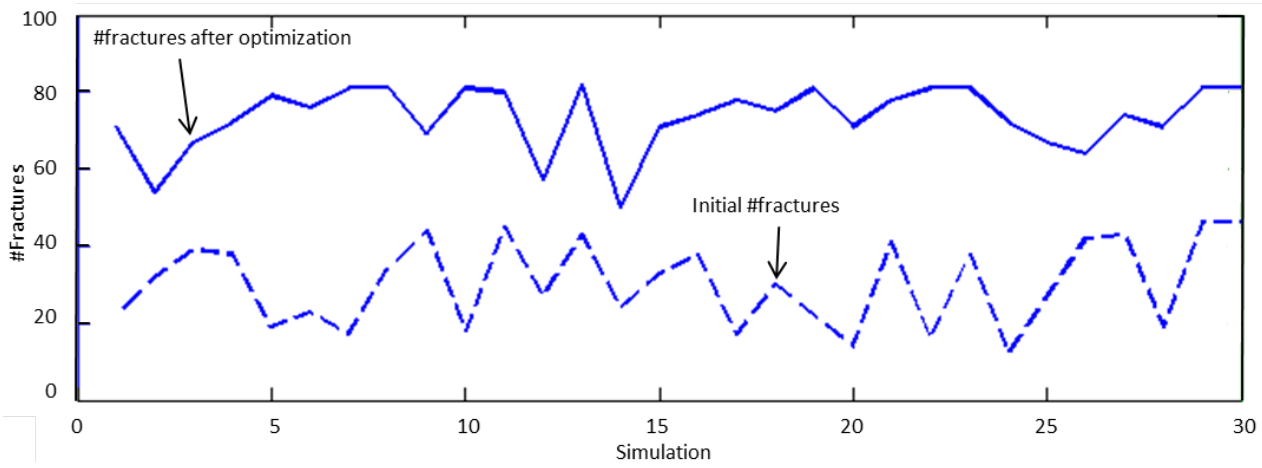

Figure 5. Number of fractures before and after optimization (10000 iterations) for 30 simulations

5.2. Habanero dataset

The Habanero wells are part of Geodynamics' HDR geothermal project in the Cooper Basin, South Australia. These wells have been drilled to depths of about 4400m below the surface or about 700m into the bedrock where temperatures reach 250°C (Baisch et al., 2006). The dataset used in this study contains a total of 23230 micro-seismic events covering an approximate area of 2.5 km^2. The absolute hypocentre locations of these events are shown in Fig. 6a, in which the colour indicates the times at which the events are detected (coloured from blue to red with increasing time).

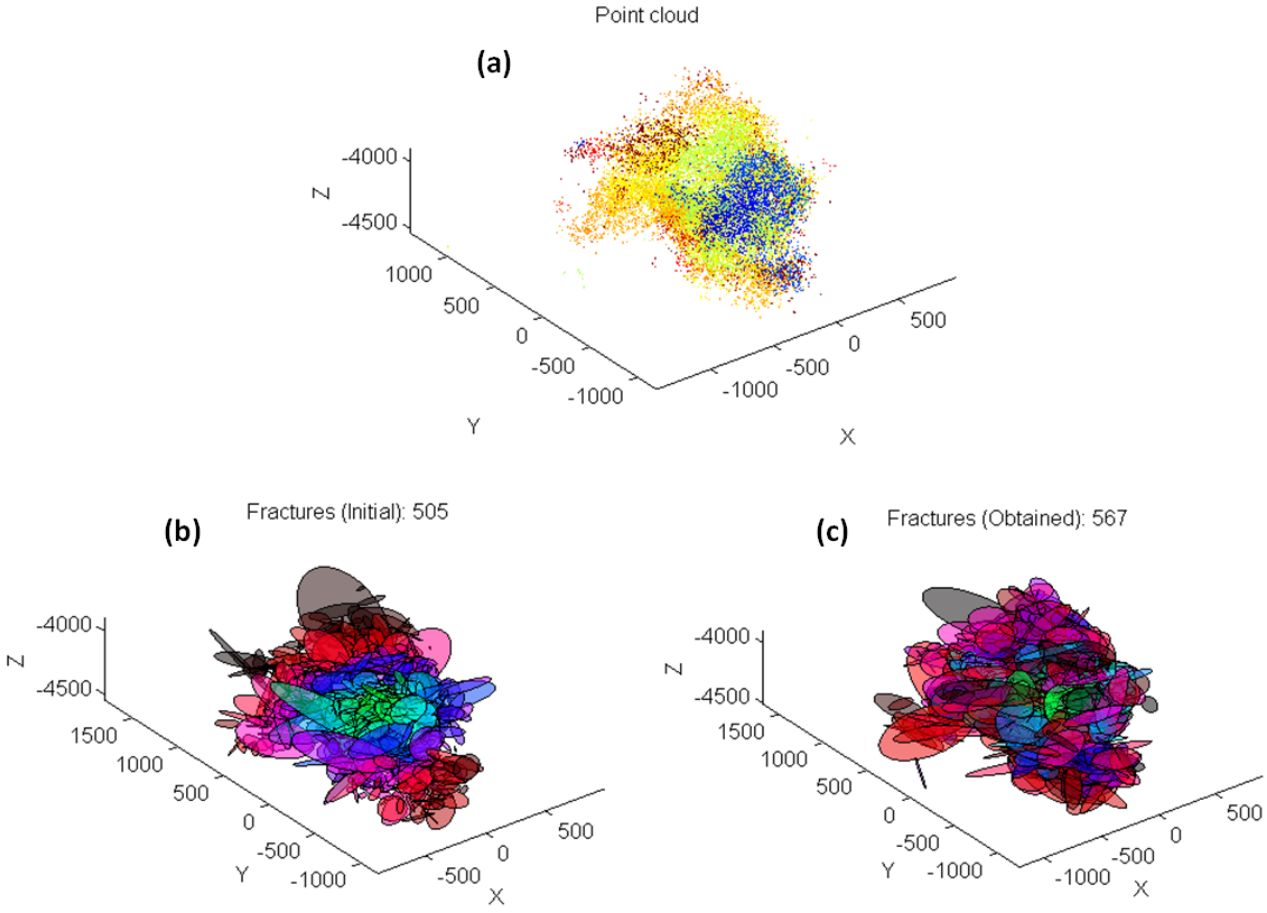

Figure 6. Habanero dataset: a) the seismic events; coloured from blue to red according with increasing time; b) the prior map; c) the final fractures obtained after optimization

Fig. 6b shows the prior map with 505 fractures which is constructed as follows. Starting from the farthest point from the borehole location (i.e. $x = y = 0$), a fracture is created if the distances of the point from the existing fractures are greater than a pre-specified threshold; here we set the threshold to 50 (proportional to the penalty for an outlier). The centre of the fracture is set as the point location and the other parameters are generated from their distributions. The mean and variance corresponding to the parameters of a lognormal distribution are set to 100 and 2000. The resulting fractures after optimization in which the temperature reached 10^{-9} (63876 iterations) are shown in Fig. 6c which is the optimal solution generated by the proposed algorithm. The number of fractures after optimization is 567 compared to 613 fractures in the work of Baisch et al. (2006) and Xu et al. (2013). The model here is an extension to the model proposed by Xu et al. (2013) in which the number of fractures is no longer fixed and varies during the optimization process. It is also an extension of our previous work (Seifollahi et al. 2012) in terms of new components for the objective function and new proposals formulated specifically for general 3D applications.

Fig. 7a and Fig. 7c show the point-fracture associations before and after optimization. The two largest fractures in Fig. 6c have associations of 424 and 511 points, while the largest fracture in Xu et al. (2013) has an association of 393 points. Fig. 7b and Fig. 7d show the distances of the points from the prior and final fracture models respectively. From final map 95 per cent of the distances are within ± 12 metres while they are ± 22.89 and ± 12.93 in our previous works, Seifollahi et al. (2012) and Seifollahi et al. (2013), respectively.

Fig. 8a shows the variation in the number of fractures against iterations. Fig. 8b, with a very similar trend to that in Fig. 8a, shows the amount of fracturing (the objective function f_2) and Fig. 8c shows the volumes of convex hulls or the objective function f_3. The total objective function values are shown in Fig. 8d in which there is a sharp decline in early iterations and stability towards the end of the process.

Fig. 9a-9b show the distributions of major and minor axes of fractures in the prior map, while Fig 9c-9d show the distributions of the same variables in the final fracture model. Fig. 9a-9f show the distributions of fracture orientations. The upper figures are for the prior map and the lower ones for the final fracture model. Fig. 10a-10c show the distribution of fracture orientations in the prior map, while the lower figures, Fig. 10d-10f, are for the final fracture model.

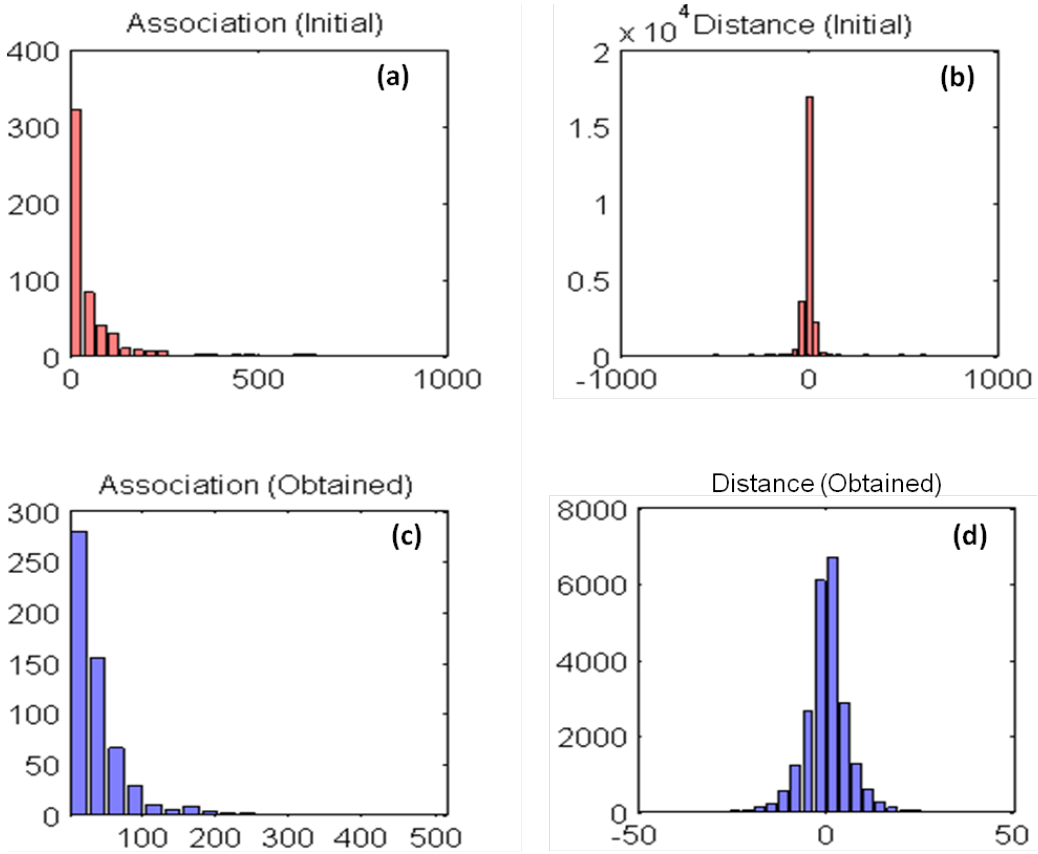

Figure 7.a)-b) Distributions of point-fracture associations (or number of points in fractures) and distances of the points from fractures in the prior map; c)-d) the same distributions in the final map

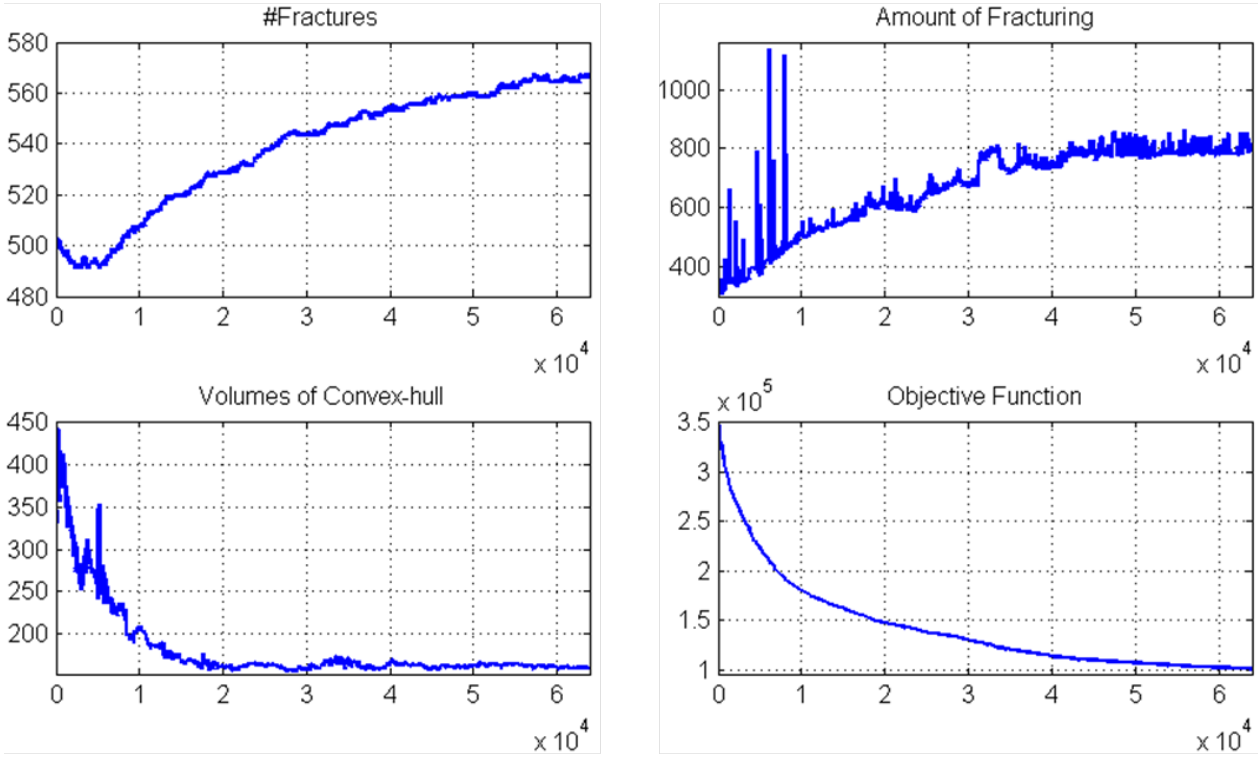

Figure 8: a) variation of number of fractures; b) amount of fracturing (f_2); c) volumes of convex hulls (f_3); d) total objective function value

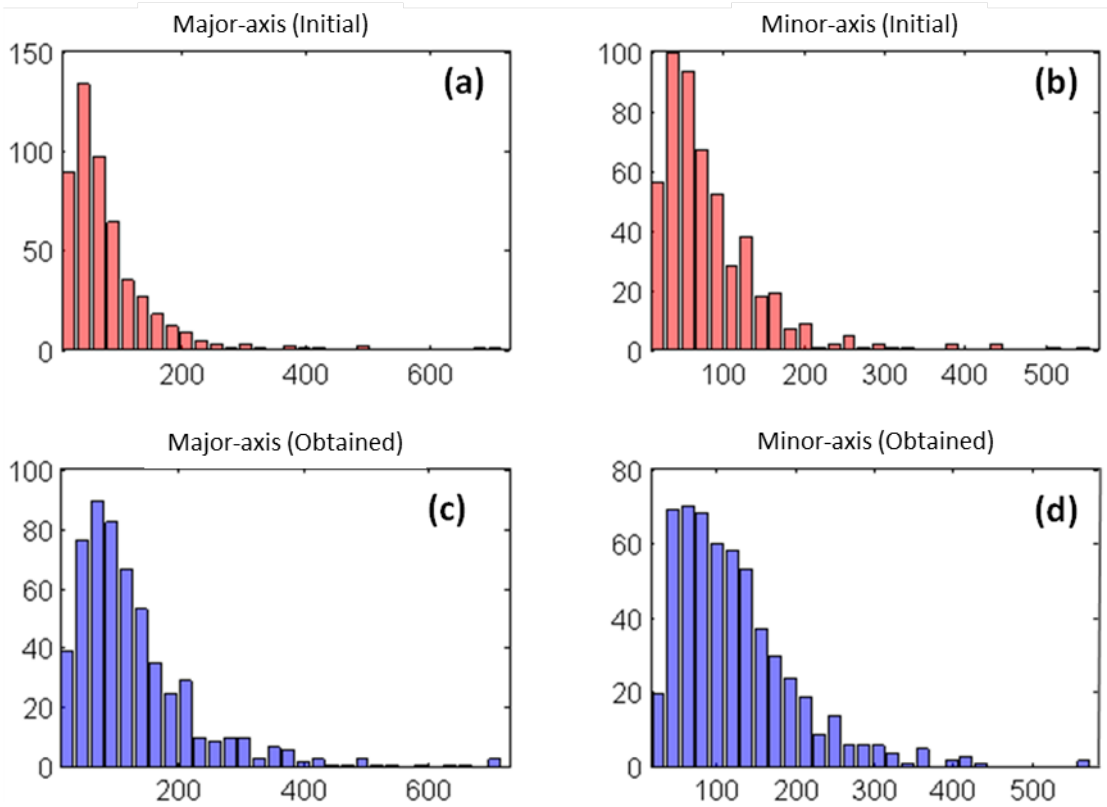

Figure 9. a)-b) Distribution of major and minor axes for the prior map; c)-d) the same distributions for final map

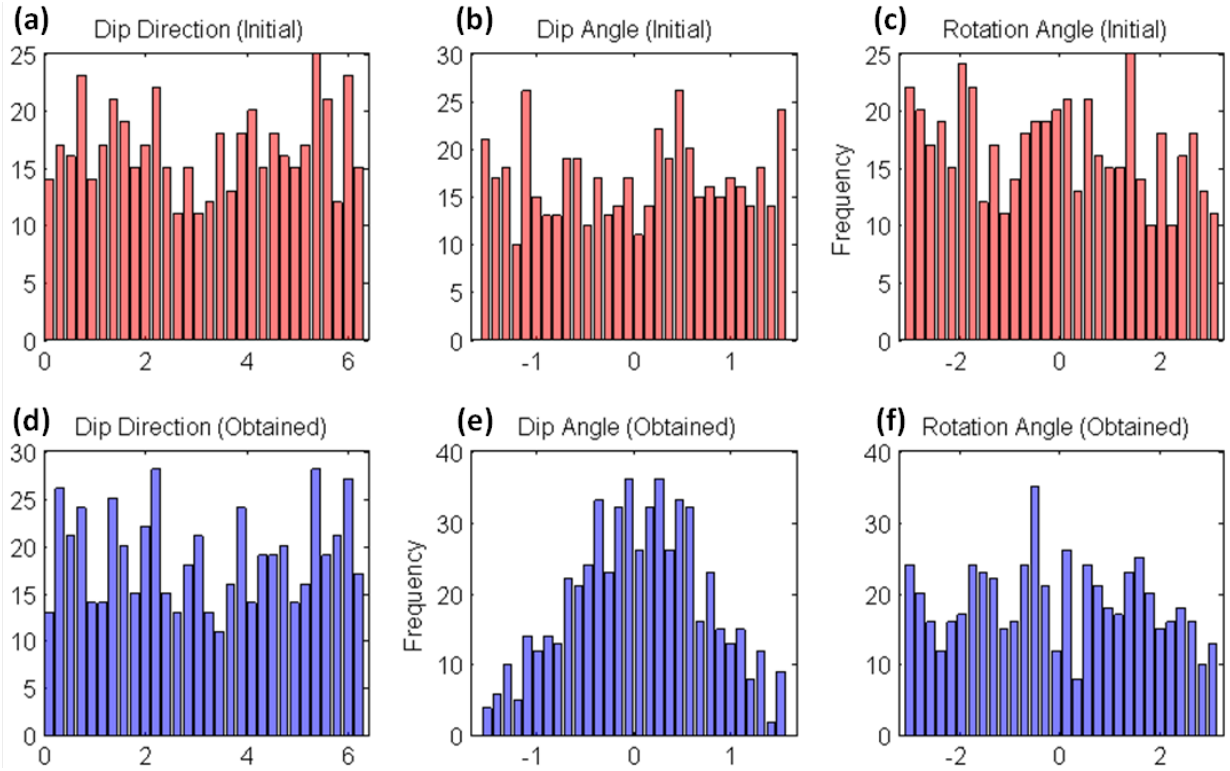

Figure 10: a)-c) Distributions of fracture orientations for the prior map; d)-f) the same distributions for the final map

For comparison of the output with that of Seifollahi et al. (2012), we ran the algorithm using 371 initial fractures by terminating the initial process when the number of initial fractures exceeded 371. The results (Figs 11a and 11b) show the variation in the number of fractures and the total objective function values against iterations. After optimization 95 per cent of the distances are within ± 11.5 metres. There is no way of knowing the number of fractures in the Habanero dataset and thus it is difficult to determine definitively which algorithm performs better due to the many uncertainties but the number of association points, the number of final fractures and the error are three important factors that quantify the effectiveness of our algorithm.

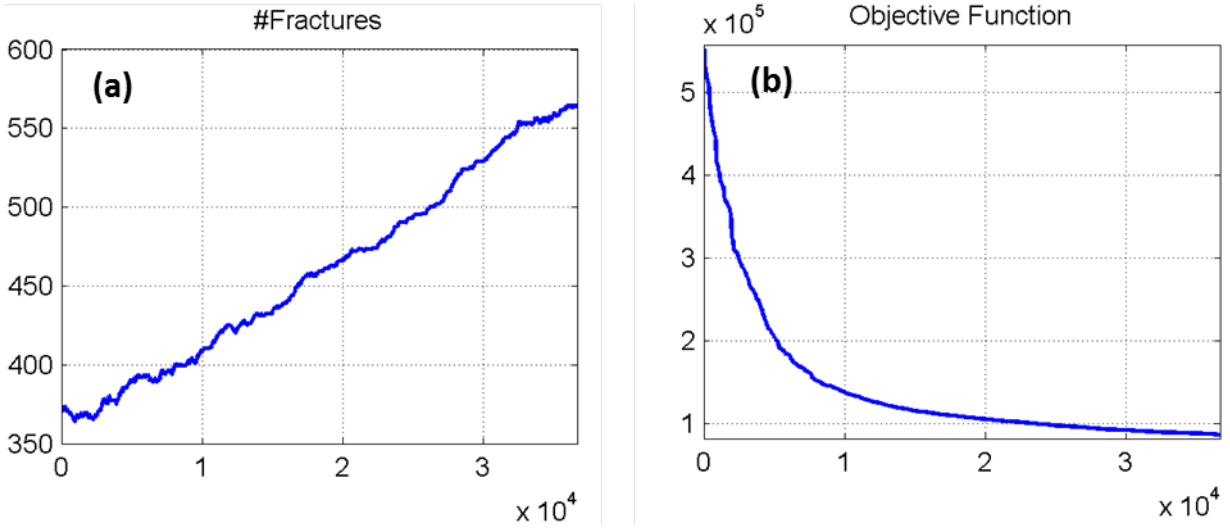

Figure 11: a) variation of number of fractures; b) total objective function value

5.3. Conclusions and future work

In the present work, we have developed a stochastic optimisation approach for fracture network modelling conditioned to the micro-seismic points derived from the fracture stimulation of a HDR geothermal reservoir. The number of association points, the number of final fractures and the error are three important factors that quantify the effectiveness of our algorithm. On the basis of these measures we conclude that the algorithm presented here is a significant extension of our previous published work in Seifollahi et al. (2012). The method has been applied to a simulated dataset and a real dataset from the Habanero reservoir. The results for both datasets are satisfactory in terms of the accuracy and the statistics of the simulated fractures.

The time domain is an important feature of the seismic events (see Fig. 6a) which indicates the propagation sequence of the fractures in the reservoir during the fracture stimulation process. Work is now underway to include the time domain of the events to improve the fracture modelling.

Acknowledgment

The work reported in this paper was funded by Australian Research Council Discovery Project Research Grant Number: DP110104766. We thank Geodynamics Limited for providing access to the micro-seismic data.

References

- Andersson J, Shapiro AM, Bear J (1984) A stochastic model of fractured rock conditioned by measured information. Water Resources Research 20:79–88
- Baecher GB, (1983) Statistical analysis of rock mass fracturing. Mathematical Geology 15 (2):329–348
- Baisch S, Weidler R., Vörös R, Wyborn D, Graaf L-de (2006) Induced seismicity during the stimulation of a geothermal HFR reservoir in the Cooper Basin, Australia. Bulletin of the Seismological Society of America, 96(6):2242–2256
- Brown D, DuTeaux R, Kruger P, Swenson D, Yamaguchi T (1999) Fluid circulation and heat extraction from engineered geothermal reservoirs. Geothermics 28:553-572
- Cressie, N (1993) Statistics for spatial data. Wiley, New York
- Dershowitz WS, Einstein HH (1988) Characterizing rock joint geometry with joint system models. Rock Mechanics and Rock Engineering 21(1):21–51
- Dershowitz W, LaPointe P (1994) Discrete fracture approaches for oil and gas applications. In: Nelson PP, Laubach SE (eds) Proceedings of the Northern American rock mechanics symposium, Austin, TX. Balkema, Rotterdam, pp 19–30
- Deutsch CV, Cockerham PW (1994) Practical considerations in the application of simulated annealing to stochastic simulation. Mathematical Geology, Vol 26, No 1
- Dowd PA, Xu C, Mardia KV, Fowell RJ (2007) A comparison of methods for the simulation of rock fractures. Mathematical Geology, 39:697-714
- Einstein HH (2003) Uncertainty in rock mechanics and rock engineering—then and now, In: Proceedings of the 10th international congress of the ISRM. The South African institute of mining and metallurgy symposium series S33, vol. 1, pp 281–293
- Fadakar, AY, Dowd PA, Xu C (2013) The RANSAC method for generating fracture networks from micro-seismic event data. Journal of Mathematical Geosciences, DOI 10.1007/s11004-012-9439-9
- Geman S, Geman D (1984) Stochastic relaxation, Gibbs distributions, and the Bayesian Restoration of Images. IEEE Transactions on Pattern Analysis and Machine Intelligence 6 (6): 721–741

- Goovaerts P (1998) Accounting for estimation optimality criteria in simulated annealing. Mathematical Geology, Vol. 30, No. 5
- Hsieh PA, Neuman SP, Stiles GK, Simpson ES (1985) Field determination of the 3-dimensional hydraulic conductivity tensor of anisotropic media 2. Methodology and application to fractured rocks. Water Resources Research 21(11):1667-1676.
- Kirkpatrick S, Gelatt-J CD, Vecchi MP (1983) Optimization by simulated annealing. Science, 220:671-680
- Long JCS, Remer JS, Wilson CR, Witherspoon PA, (1982) Porous media equivalents for networks of discontinuous fractures. Water Resources Research 18(3):645–658
- Long JCS, Witherspoon PA (1985) The relationship of the degree of interconnection to permeability in fracture networks. J Geophys Res B 90(4):3087-3098
- Mardia KV, Nyirongo VB, Walder AN, Xu C, Dowd PA, Fowell RJ, Kent JT (2007a) Markov Chain Monte Carlo implementation of rock fracture modelling. Mathematical Geology, 39:355-381
- Mardia KV, Walder AN, Xu C, Dowd PA, Fowell RJ, Nyirongo VB, Kent JT (2007b) A line finding assignment problem and rock fracture modelling. Bayesian Statistics and its Applications, Eds. Upadhaya, S.K., Singh, U., Dey, D.K. (Eds), Anamaya Pubs, New Delhi pp 319-330
- Nelson RA (1982) An approach to evaluating fractured reservoirs. SPE10331, SPE J. Petrol. Technol., September
- Odling NE (1992) Permeability and simulation of natural fracture patterns, in Structural and Tectonic modelling and its application to petroleum geology. Nor Pet Soc Spec Publ 1:365–380
- Robinson PC (1983) Connectivity of fracture systems-a percolation theory approach. Journal of Physics A: Mathematical and General 16:605–614
- Sahimi M (1993) Flow phenomena in rocks: from continuum models to fractals, percolation, cellular automata and simulated annealing. Reviews of Modern Physics 65 (4):1393–1534
- Seifollahi S, Dowd PA, Xu C (2012) A stochastic model for the fracture network in the Habanero enhanced geothermal system. Proceedings of the 2012 Australian Geothermal Energy Conference 2012, Sydney
- Seifollahi S, Dowd PA, Xu C, Fadakar AY (2013) A Spatial Clustering Approach for Stochastic Fracture Network Modelling. Rock Mech Rock Eng DOI 10.1007/s00603-013-0456-x
- Tamagawa T, Matsuura T, Anraku T, Tezuka K, Namikawa T (2002) Construction of Fracture Network Model Using Static and Dynamic Data. Society of Petroleum Engineers Annual Technical Conference and Exhibition. Texas, USA
- Tran NH, Chen Z, Rahman SS (2007) Practical application of hybrid modelling to naturally fractured reservoirs. Petroleum Science and Technology, 25:1263-1277
- Tran NH, Rahman MK, Rahman SS (2002) Developing a hot dry rock reservoir in Australia by hydraulic stimulation: a shear-dilation model for design and evaluation. Geothermal Resources Council Transactions 26
- Xing, H, Zhang, J, Liu, Y, Mulhaus, H (2009) Enhanced geothermal reservoir simulation. Proceedings of the Australian Geothermal Energy Conference 2009, Brisbane
- Xu, C and Dowd, PA (2010) A new computer code for discrete fracture network modelling. Computers and Geosciences, 36:292-301
- Xu C, Dowd PA, Mardia KV, Fowell RJ (2006) A connectivity index for discrete fracture networks. Mathematical Geology, 38:611-634
- Xu C, Dowd PA, Mardia KV, Fowell RJ, Taylor CC (2007) Simulating correlated marked point processes. Journal of Applied Statistics, 34:1125-1134
- Xu C, Dowd PA, Wyborn D (2013) Optimization of a stochastic rock fracture model using Markov Chain Monte Carlo Simulation. Mining Technology, 122(3):153-158.